Intelligent Prediction of The Equivalent Circulating Density From Surface Data Sensors During Drilling By Employing Machine Learning Techniques

Hany Gamal (g201706870@kfupm.edu.sa)
King Fahd University of Petroleum and Minerals
Ahmed Abdelaal
King Fahd University of Petroleum and Minerals
Salaheldin Elkatatny
King Fahd University of Petroleum and Minerals

Research Article

Keywords: Equivalent circulating density, real-time, drilling parameters, artificial intelligence

Posted Date: February 5th, 2021

DOI: https://doi.org/10.21203/rs.3.rs-154257/v1

Intelligent Prediction of the Equivalent Circulating Density from Surface Data Sensors During Drilling by Employing Machine Learning Techniques

Hany Gamal
Ph.D. Candidate
Department of Petroleum Engineering,
King Fahd University of Petroleum & Minerals,
Dhahran 31261, Saudi Arabia; Box: 5049
g201706870@kfupm.edu.sa

Ahmed Elsayed Abdelaal
Ph.D. Student
Department of Petroleum Engineering,
King Fahd University of Petroleum & Minerals,
Dhahran 31261, Saudi Arabia; Box: 5049
g201708850@kfupm.edu.sa

Salaheldin Elkatatny*
Department of Petroleum Engineering,
King Fahd University of Petroleum & Minerals,
Dhahran 31261, Saudi Arabia; Box: 5049
elkatatny@kfupm.edu.sa

*Corresponding Author: elkatatny@kfupm.edu.sa

Intelligent Prediction of the Equivalent Circulating Density from Surface Data Sensors During Drilling by Employing Machine Learning Techniques

Hany Gamal[1], Ahmed Abdelaal[1], Salaheldin Elkatatny[1]*

[1] College of Petroleum Engineering and Geosciences, King Fahd University of Petroleum & Minerals, 31261 Dhahran, Saudi Arabia. g201706870@kfupm.edu.sa (H.G.), g201708850@kfupm.edu.sa (A.AB), elkatatny@kfupm.edu.sa (S.E.)

* Corresponding Author. elkatatny@kfupm.edu.sa; Tel.: +966-594663692

Abstract: The precise control for the equivalent circulating density (ECD) will lead to evade well control issues like loss of circulation, formation fracturing, underground blowout, and surface blowout. Predicting the ECD from the drilling parameters is a new horizon in drilling engineering practices and this is because of the drawbacks of the cost of downhole ECD tools and the low accuracy of the mathematical models. Machine learning methods can offer a superior prediction accuracy over the traditional and statistical models due to the advanced computing capacity. Hence, the objective of this paper is to use the artificial neural network (ANN) and adaptive neuro-fuzzy inference system (ANFIS) techniques to develop ECD prediction models. The novel contribution for this study is predicting the downhole ECD without any need for downhole measurements but only the available surface drilling parameters. The data in this study covered the drilling data for a horizontal section with 3,570 readings for each input after data preprocessing. The data covered the mud rate, rate of penetration, drill string speed, standpipe pressure, weight on bit, and the drilling torque. The data used to build the model with a 77:23 training to testing ratio. Another data set (1,150 data points) from the same field was used for models` validation. Many sensitivity analyses were done to optimize the ANN and ANFIS model parameters. The prediction of the developed machine learning models provided a high performance and accuracy level with a correlation coefficient (R) of 0.99 for the models' training and testing data sets, and an average absolute percentage error (AAPE) less than 0.24%. The validation results showed R of 0.98 and 0.96 and AAPE of 0.30% and 0.69% for ANN and ANFIS models respectively. Besides, a mathematical correlation was developed for estimating ECD based on the inputs as a white-box model.

***Keywords*:** Equivalent circulating density; real-time; drilling parameters, artificial intelligence

1. Introduction

Equivalent circulating density is an important parameter for monitoring the drilling operations especially for the narrow window between the formation and the fracture pressure. ECD is the total pressure of the mud hydrostatic column and the annular losses, and hence, it shows the mud pressure against the formation in the case of mud circulation[1]. Therefore, it is critical to estimate the ECD with a high degree of precision to avoid any well control issues like loss of circulation, formation fracturing, and underground blowout situations.

During the drilling operations, several factors were found to have an impact on the ECD, and among them, the annular pressure losses, wellbore geometry, mud properties (density and viscosity), mud pumping rate, downhole pressure and temperature, and concentration of cuttings [2-5].

ECD can be acquired by means of downhole measurements, estimation using mathematical models, and/or predicting with the help of artificial intelligence (AI) techniques. The new technology in the drilling tools assisted in implementing a continuous circulating tool to monitor the ECD and provide good control for the formation pressure [6]. Downhole measurements of the ECD are available using downhole sensors as measurements while drilling and pressure while drilling [7,8]. The downhole measurement is considered accurate and robust for ECD values, however, the implementation of these downhole tools is not common due to the expensive daily charge and operational limitations such as downhole pressure and temperature that cause the tool failures.

Several mathematical correlations exist in the literature for estimating the ECD that are different in the fluid type and the parameters utilized as inputs. ECD estimation by implementing the material balance calculation for

the mud compositional analysis was studied in the literature [9,10]. However, the models had many assumptions and limitations regarding the downhole pressure, temperature, mud types. Bybee [11] introduced a mathematical equation to calculate the ECD. The model considers the effect of concentration of solids in the annular, in addition to, the mud static density and other mud-related parameters.

The developed mathematical correlations are limited to some applications, and it ignores a lot of other input parameters that have an impact on the ECD values. Such ignored parameters as well geometry, fluid rheological properties, the rotation of the drill string, downhole pressure and temperature conditions that affect the mud density, cuttings dispersion, hole cleaning, and swab and surge of drillpipe movements in the hole [12,13]. Ignoring these parameters will affect the ECD prediction and lead to the inaccurate evaluation of ECD and causes well control problems during the drilling operations [14,15].

1.1. Predicting ECD by Employing Machine Learning Techniques

Predicting the ECD from the drilling parameters is considered a new outlook for drilling engineering practices in the petroleum industry and that because of the limitations of the downhole ECD tools and the low accuracy of the mathematical models.

Artificial intelligence is a technique that utilized high computing capabilities for processing advanced algorithms to solve technical/problematic issues by simulating the human brain's thinking manner [16]. AI has many tools like artificial neural networks (ANNs), adaptive neuro-fuzzy inference system (ANFIS), support vector machine (SVM), and functional networks (FN) that showed high performance and accuracy level for prediction and classification problems [17]. The implementation of AI has wide applications in many disciplines of engineering, economics, medicine, military, marine sectors, etc. [18,19].

In the oil and gas industry, many studies utilized machine learning techniques for finding solutions for practical challenges [20-23]. Intelligent models were accomplished by artificial intelligence tools for many purposes as identifying the formation lithology [24], predicting the formation and fracture pressures [25, 26], estimating the properties of reservoir fluids [27], estimating the oil recovery factor [28, 29], predicting the tops of the drilled formation [30], ROP prediction and optimization for different drilled formations and well profiles [31-33], determining the content of total organic carbon [34-36], and estimating the rock static Young's modulus [37-40], predicting the compressional and shear sonic times [41], determining the rock failure parameters 42, detecting the downhole abnormalities during horizontal drilling [43], determining the wear of a drill bit from the drilling parameters [44], and predicting the rheological properties of drilling fluids in real-time [45-49].

For ECD prediction, Table 1 represents recent works that were performed for ECD prediction from the drilling and mud parameters. Ahmadi [50] utilized the least square support vector machine (LLSVM), ANFIS, and enhanced particle swarm optimization PSO-ANFIS tools to estimate the ECD from only mud initial density, pressure, and temperature. The results showed the outperformance of ANN than the other tools. Ahmadi et al. [51] studied predicting ECD by employing PSO-ANN, fuzzy inference system (FIS), and a hybrid of genetic algorithm (GA) and FIS (GA-FIS) from the initial mud density, pressure, and temperature data. The PSO-ANN model presented a high degree of prediction performance in terms of coefficient of determination (R^2) and average absolute percentage error between the actual and predicted values of ECD.

Alkinani et al. [52] predicted the ECD using the ANN model that had only one hidden layer and 12 neurons and the study utilized drilling parameters in addition to the hydraulics and mud properties as mud pumping rate, properties of the mud (density, plastic viscosity, and yield point), total flow area for the bite nozzles (TFA), revolutions per minute for the drill pipe (RPM), and the weight on bit (WOB). Abdelgawad et al. [5] provided a model for ECD prediction using two AI techniques ANN, and ANFIS. The study provided an ECD-ANN model of one hidden layer with 20 neurons, while the ANFIS model was developed by utilizing five membership functions with gaussian membership function (gaussmf) as the input membership function and the output membership function was a linear type. Rahmati and Tatar [53] employed radial basis function (RBF) to build an ECD prediction model that showed a good prediction capability with R^2 of 0.98 and AAPE of 0.22%.

Table 1. ECD prediction models using AI among the literature

Ref.	Model	Model Inputs	Data	R^2	AAPE
Ahmadi [50]	LSSVM	Pressure Temperature Initial density	Not Available	0.9999	0.000145
	ANFIS			0.8502	35.002
	PSO-ANFIS			0.869	Not Available
Ahmadi et al. [51]	PSO-ANN	Pressure Temperature Initial density	664 points from literature	0.9964	0.0001374
	FIS			0.7273	67.0907
	GA-FIS			0.9397	0.091
Alkinani et al. [52]	ANN	Flow rate Mud weight Plastic viscosity Yield point TFA RPM WOB	2000 wells	0.982	Not Available
Abdelgawad et al [5]	ANFIS	Mud weight Drill pipe pressure ROP	2376 data points 8.5″ vertical hole section	0.98	0.22
	ANN				
Rahmati and Tatar [53]	Radial Basis Function (RBF)	Pressure Temperature Type of mud Initial density	884 points from literature	0.99	MSE 0.00000166

It is clear from the literature that the AI models enhanced the ECD prediction, however, the models are different in terms of the input parameters, the data used to feed the models, and the methodology followed for the ECD prediction. One of the shortcomings found from many studies in the literature is that the downhole pressure and temperature are required as inputs in the prediction models, and from an operational view, downhole sensors are required to acquire these parameters with high accuracy for better ECD prediction, and this will add operational cost and time for the data collecting. Consequently, the new contribution of this study is to employ available real-time drilling parameters from surface rig sensors to build ECD prediction models using ANN and ANFIS techniques.

The novel approach in this study is that the AI models are mainly dependent only on the mechanical drilling parameters that are mud pumping rate (GPM), rate of penetration (ROP), drillstring speed in revolutions per minute (RPM), stand-pipe pressure (SPP), weight on bit (WOB), and drilling torque (T). Besides, the study presented an empirical correlation that can be easily utilized for ECD estimation from only the drilling parameters. The AI models that were presented in this study were validated from another data set to ensure high and robust performance for ECD prediction.

2. Materials and Methods

The study utilized real drilling data that was collected from the drilling operations from real-time sensors. Figure 1 represents, in brief, the processing flow to provide robust ECD models starting from the data gathering, data cleaning and filtering to provide the model input parameters with good quality, the training process for the AI model and optimizing the model parameters with the trained algorithm, testing the accuracy for the model results and if the accuracy is low, then re-training process should be performed in order to get the optimum model parameters for high accuracy performance for the ECD prediction.

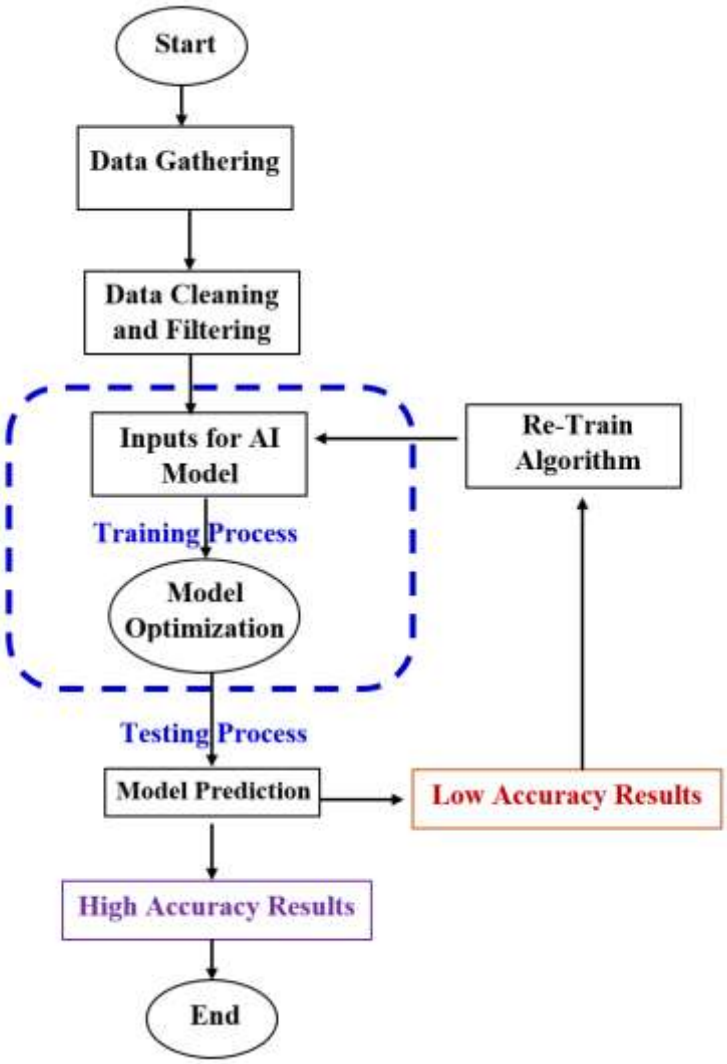

Figure 1: Processing flow chart for ECD AI models.

2.1 Data Description

The data obtained for the current study was collected during a drilling phase in the Middle East. The data covered the horizontal section for drilling the 5-7/8-inch hole. Total 3,570 points were obtained after the data preprocessing. The drilling parameters that were utilized as inputs for the model were collected from the surface rig sensors that represent GPM, ROP, RPM, SPP, WOB, and T. ECD data was collected from the downhole pressure tool and it was used for the model output estimation. Also, another cleaned data set (1,150 points) from the same drilling phase was employed for further model validation as unseen data set to ensure the model prediction performance.

2.2 Data Cleaning and Statistical Analysis

The obtained data are preprocessed by removing the missing points and the data outliers using MATLAB. As shown in Figure 2, the correlation coefficients (R) between the output (ECD) and drilling parameters after preprocessing the data. The relative importance of the data showed that SPP and T have the highest R of 0.87 and 0.85 respectively with the ECD, while the WOB showed the least R (-0.01) with the ECD and that shows that the relationship might be a nonlinear type between ECD and WOB. It is noticed that T, SPP, and RPM showed a direct relationship with ECD, while GPM, ROP, and WOB presented an indirect relationship with ECD.

Table 2 shows the statistical analysis for all parameters. The data showed the wide range for the parameters as GPM ranged from 249.4 to 296.6 with 47.2 gallons-per-minutes (gpm), ROP from 3.5 to 59.6 ft/hr, SPP from

2,379.7 to 3,632.1 psi, RPM from 59 to 141.3 revolutions-per-minute, T from 3.7 to 10 kft.Ib, WOB from 5.5 to 20 kIb, and ECD has a range of 12.1 pcf from a minimum value of 83.4 to a maximum value of 95.5 pcf.

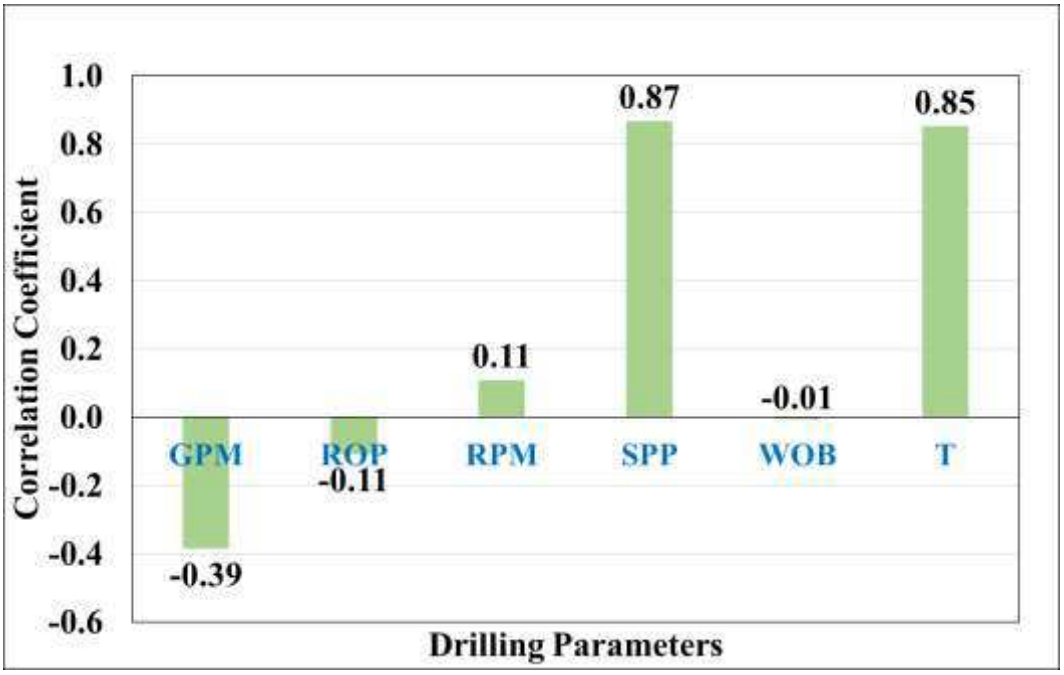

Figure 2. The correlation coefficients between the inputs and ECD after data preprocessing

Table 2. Statistical analysis for the models' data.

Statistical Parameter	GPM	ROP (ft/hr)	RPM	SPP, psi	WOB (klb)	T (kft.Ib)	ECD, pcf
Minimum	249.4	3.5	59.0	2379.7	5.5	3.7	83.4
Maximum	296.6	59.6	141.3	3632.1	20.0	10.0	95.5
Range	47.2	56.1	82.3	1252.4	14.6	6.3	12.1
Mean	276.7	23.0	119.8	3035.3	15.2	6.9	90.4
Median	281.0	23.7	120.0	3032.7	16.1	6.9	90.4
Standard Deviation	10.3	6.2	16.9	258.0	3.0	1.2	3.2
Kurtosis	1.11	1.88	1.28	-0.14	0.08	-0.87	-0.89
Skewness	-1.67	0.22	-0.93	-0.15	-0.96	-0.05	-0.39

2.3 Building AI Models

This study employed two techniques from the AI tools to develop ECD prediction models using only the drilling parameters. ANN and ANFIS techniques are trained using the input data by training and testing ratio of 77 to 23. The training and testing data sets were randomly selected. The sensitivity analysis for each model parameter to have the best model architecture. The model prediction was evaluated with two statistical parameters in addition to the ECD profiles for the actual and the predicted data. The correlation coefficient (R) and the average absolute percentage error (AAPE) were calculated by Equations 1 and 2.

$$AAPE = \left(\frac{1}{N}\sum_{i=1}^{N}\left|\frac{Y_i-\hat{Y}_i}{Y_i}\right|\right) x\ 100 \qquad (1)$$

$$R = \frac{N\left(\sum_1^N Y_i\hat{Y}_i\right)-\left(\sum_1^N Y_i\right)\left(\sum_1^N \hat{Y}_i\right)}{\sqrt{\left[N\sum_1^N Y_i^2-\left(\sum_1^N Y_i\right)^2\right]\left[n\sum_1^N \hat{Y}_i^2-\left(\sum_1^N \hat{Y}_i\right)^2\right]}} \qquad (2)$$

where N is the number of samples in the dataset, Y_i is the actual output, $\widehat{Y}_i$ is the predicted output.

2.3.1 Artificial Neural Network (ANN) Model

ANN tool was utilized for solving engineering problems by its processing algorithms based on interconnected artificial neurons that mimic the biological neural networks [54,55]. Three layers represented the common architecture for ANN which are the input layer, hidden layer, and output layer [56]. These layers are connected by a set of weights and biases which are tuned during the optimization process of the network to control the prediction performance of the network [57]. The network is usually trained with different learning algorithms to optimize the network and to control the processing of the neurons [58]. These neurons are considered the elementary elements from which any neural network is constructed [59].

Many parameters were tested to check its impact on the ANN model accuracy as the hidden layer/s number, the neurons` number, network, training, and transfer functions. Figure 3 shows the design of the developed ANN model in this study.

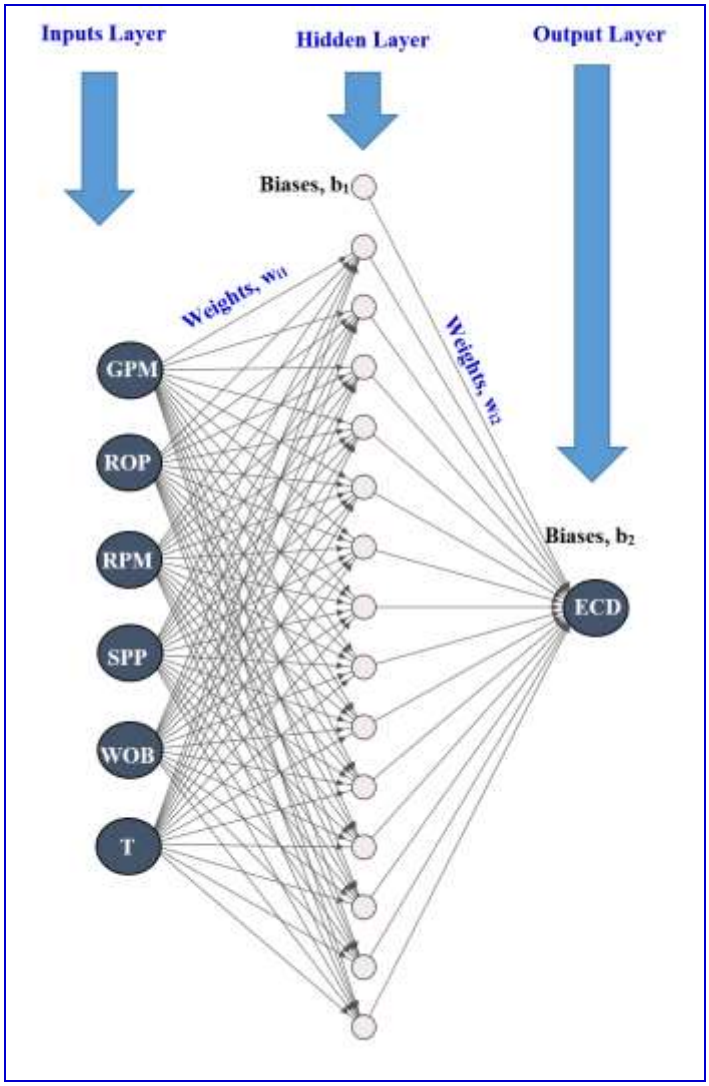

Figure 3. The architecture of the developed ANN model.

2.3.2 Adaptive Neuro-Fuzzy Inference System (ANFIS) Model

ANFIS is an adaptive neuro-fuzzy inference system that was established in the early 1990s [47]. ANFIS is a type of ANN that depends on the Takagi–Sugeno fuzzy inference system [60]. The interface of ANFIS utilized a set of fuzzy "if-then rules" that can learn and optimize the nonlinear functions [61]. ANFIS architecture consists of four layers. The first layer, called the fuzzification layer, collects the inputs and determines the membership functions (e.g. sigmoid, gaussian, trapezoidal, or straight line). The second layer, denoted as "rule layer", applies many fuzzy "if-then" rules. In the third layer, databases are employed for membership function rules, and the decision-making unit is developed for the inference operations, while in the last layer, the defuzzification interface is performed [61].

ANFIS model was developed using the subtractive clustering method. The cluster radius and number of iterations are ANFIS parameters that were checked for the optimization process.

3. Results and Discussion:

This section discussed the obtained results from the two AI developed models for predicting the ECD from the real-time drilling parameters.

3.1 ANN Results

The designed ANN code was optimized by testing many scenarios to achieve the best model parameters that are listed in Table 3. For each code run, only one parameter option was tested and the results were compared in terms of R and AAPE. By the end of the optimization process, the best combination of the model parameters was recognized. Training to testing ratio for the data sets was found to be 77 to 23% as 2,743 data points for training and 827 points of data for the testing process, only one hidden layer with 15 neurons was efficient for better prediction accuracy, the best network, training, and transfer functions were fitting network (newfit), Levenberg-Marquardt backpropagation (trainlm), and softmax respectively, and 0.12 is the optimum learning rate.

Table 3. Tested options for ANN parameters.

Model Parameter	Options		
Training/Testing ratio	(70/30) – (90/10)		
Hidden layers	1 - 3		
Number of neurons	5 - 40		
Network Function	fitnet	newfit	newcf
	newelm	newlrn	newpr
	newdtdnn	newff	
	newfftd	newfit	
Training Function	trainbr	trainoss	trainlm
	trainbfg	traingdx	
Transfer Function	tansig	satlin	purelin
	logsig	netinv	softmax
	hardlims	radbas	tribas
Learning Rate	0.01 – 0.9		

Figure 4 represents the cross-plots for the ANN results for the model training and testing processes for estimating ECD values. the results showed a strong accuracy for the model in terms of R and AAPE for both training and testing as R was 0.99 between the real and predicted values for the ECD for training and testing, while the AAPE was 0.24 and 0.19 for training and testing respectively.

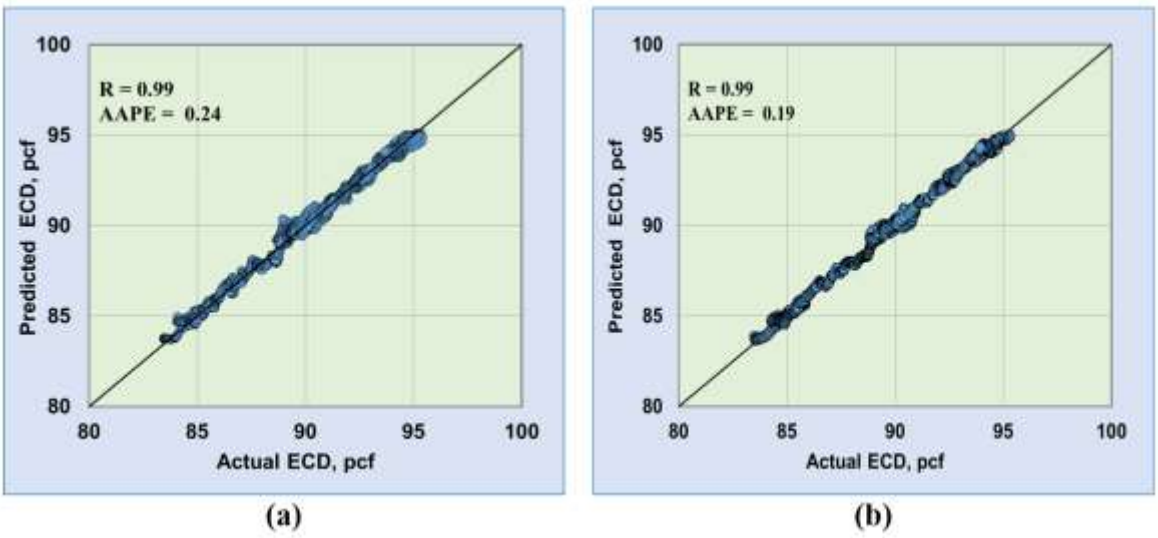

Figure 4. Cross-plots between the predicted and actual ECD results from the developed ANN model. (a) training process, and (b) testing process.

3.2 ANFIS Results

The same procedures were followed for optimizing the model parameters, however, cluster radius and iterations number are the target parameters for the ANFIS model. After several runs for the ANFIS code, the optimum parameters were found as 0.8 for the cluster radius and 300 for the number of iterations. Figure 5 displays the ANFIS results for the model training and testing processes.

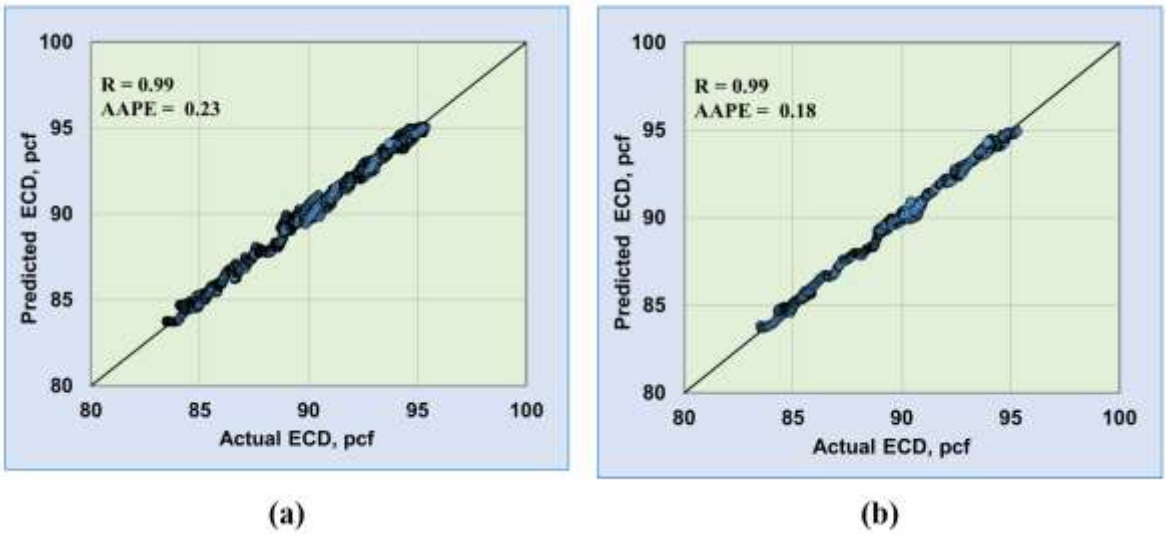

Figure 5. Cross-plots between the predicted and actual ECD results from the developed ANFIS model. (a) training process, and (b) testing process.

3.3 ECD Empirical Correlation from ANN model

An empirical correlation was developed for ECD estimation from the ANN model. The empirical correlation that can be employed to estimate the ECD using the input/drilling parameters and the weights and biases of the optimized ANN model. The developed empirical correlation can be used after normalizing the inputs to be in the range between -1 and 1 (Equation 3):

$$X_{i_{nor}} = 2 * \left(\frac{X_i - X_{i\,min}}{X_{i\,max} - X_{i\,min}}\right) - 1 \qquad (3)$$

Where, $X_{i_{nor}}$ is the normalized value for variable X, X_i is the value of variable X at point i, $X_{i\,min}$ is the minimum value of variable X, $X_{i\,max}$ is the maximum value of variable X.

The minimum and maximum values for each parameter that are used for data normalization are presented in Table 4.

Table 4: Minimum and maximum values for data normalization.

Statistical Parameter	GPM	ROP (ft/hr)	RPM	SPP, psi	WOB (klb)	T (kft.Ib)	ECD, pcf
Minimum	249.4	3.5	59.0	2379.7	5.5	3.7	83.4
Maximum	296.6	59.6	141.3	3632.1	20.0	10.0	95.5

The proposed empirical correlation that can be used for ECD estimation in the normalized form is presented in Equation 4. The correlation uses the weights and biases that are shown in Table 5.

$$ECD_{n_i} = \frac{e^{\left(w_{1_{i,1}}(GPM_n)+w_{1_{i,2}}(ROP_n)+w_{1_{i,3}}(RPM)+w_{1_{i,4}}(SPP_n)+w_{1_{i,5}}(WOB_n)+w_{1_{i,6}}(T_n)+b_{1_i}\right)}}{\sum_{i=1}^{N} w_{2_i} * e^{\left(w_{1_{i,1}}(GPM_n)+w_{1_{i,2}}(ROP_n)+w_{1_{i,3}}(RPM)+w_{1_{i,4}}(SPP_n)+w_{1_{i,5}}(WOB_n)+w_{1_{i,6}}(T_n)+b_{1_i}\right)}} + b2 \qquad (4)$$

where, ECD_{n_i} is the normalized ECD, N is the number of neurons in the hidden layer, i.e. 15, w_{1_i} is the weight associated with each feature between the input and the hidden layers, w_{2_i} is the weight associated with each feature between the hidden and the output layers, b_{1_i} is the bias associated with each neuron in the hidden layer, b_2 is bias of the output layer.

The obtained ECD_{n_i} has to be to an actual ECD value, Equation 5 can be used:

$$ECD = \frac{ECD_n + 1}{0.165289} + 83.4 \qquad (5)$$

Where, ECD_n is the normalized ECD obtained from the developed correlation, ECD is the actual value (pcf).

Table 5: Weights and biases of the developed correlation (Equation 4).

Neuron index (i)	w_1						w_2	b_1	b_2
	$w_{1_{i,1}}$	$w_{1_{i,2}}$	$w_{1_{i,3}}$	$w_{1_{i,4}}$	$w_{1_{i,5}}$	$w_{1_{i,6}}$			
1	-1.559	-0.878	-2.469	3.728	0.660	-2.934	3.901	1.884	-0.026
2	3.088	0.828	1.482	3.334	-0.876	-1.382	-1.166	1.305	

3	-0.577	-1.107	-0.642	2.227	0.848	-2.301	3.085	0.829	
4	-0.076	-0.686	2.224	2.787	0.975	-1.588	0.801	1.060	
5	0.181	-0.235	-1.104	1.483	-0.730	0.405	-1.537	0.537	
6	-1.279	-0.522	1.184	0.989	0.620	-1.746	1.699	-5.514	
7	-0.981	-3.708	1.505	-8.456	2.125	10.371	-4.956	0.692	
8	-0.268	1.731	-0.115	2.784	-1.303	1.669	-2.400	0.955	
9	-2.256	-0.347	0.825	2.623	0.254	0.474	2.534	1.094	
10	-1.321	-3.258	-0.466	0.450	-2.555	1.615	0.123	0.894	
11	2.167	2.173	0.892	-3.128	-3.853	3.017	-0.267	-0.529	
12	-0.547	-1.064	-2.841	1.685	0.678	-3.148	3.996	-1.138	
13	-3.168	-0.030	5.446	-0.513	0.475	-2.106	-1.710	1.673	
14	-3.154	-0.168	-0.546	-1.528	0.964	1.559	-1.091	-1.259	
15	8.828	0.759	-1.846	-1.541	-0.845	-0.325	-1.753	-0.952	

3.4 Models Validation

The validation process for the developed models is essential especially for the practical operations in the oil and gas industry. The developed ANN and ANFIS models were validated to ensure the models' performance for predicting the ECD for unseen data. An unseen data set (1,150 points) from the same field was collected and cleaned to be fed to the models as inputs to estimate the ECD and compare the actual versus the predicted ECD from the models. Figure 6 represents the ECD prediction performance from the two developed models. ANN model provided a higher accuracy level than ANFIS, however, the two models showed a high ECD prediction that shows a correlation coefficient of 0.98 and 0.96, and AAPE of 0.3 and 0.69 for ANN and ANFIS respectively.

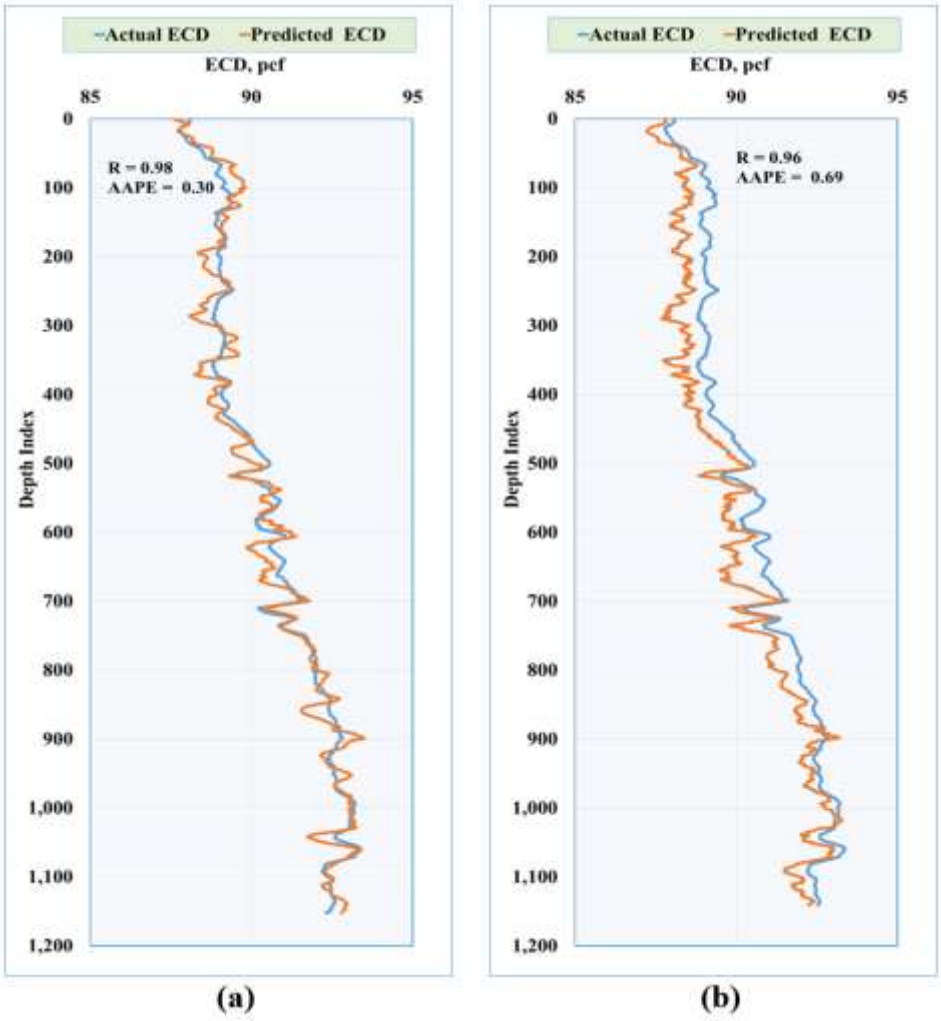

Figure 5. ECD Profile for the validation data set. (a) ANN model, and (b) ANFIS model.

3.5 Comparison of the Models Performance

The two developed machine learning techniques showed a strong performance for the ECD prediction. However, ANN outperformed the ANFIS model especially for the validation process as the slight underestimating for the ECD prediction from the ANFIS model. Figure 6 shows the error histogram for the two models for the three stages (training, testing, and validation). Both models have a slight normal distribution for the errors for training and testing that ranged between -0.4 to 0.6 (pcf). The validation process showed different distribution for the histogram of the errors as ANN had a normal distribution with a range from -0.4 to 0.8 (pcf), while ANFIS showed a range for the errors between 0 to 1 (pcf) and this is attributed to the underestimating of the ECD.

In addition, Figure 7 summarizes the performance of the two developed models in terms of the correlation coefficients and average absolute percentage error between the actual and predicted ECD values for Training, testing, and validation data sets. It is clear that the ANN model has a better performance that ANFIS for estimating ECD for the validation process as ANN provided a correlation coefficient of 0.98 while ANFIS had 0.96, and for the AAPE, ANN had 0.3% while it was 0.69% for the ANFIS model.

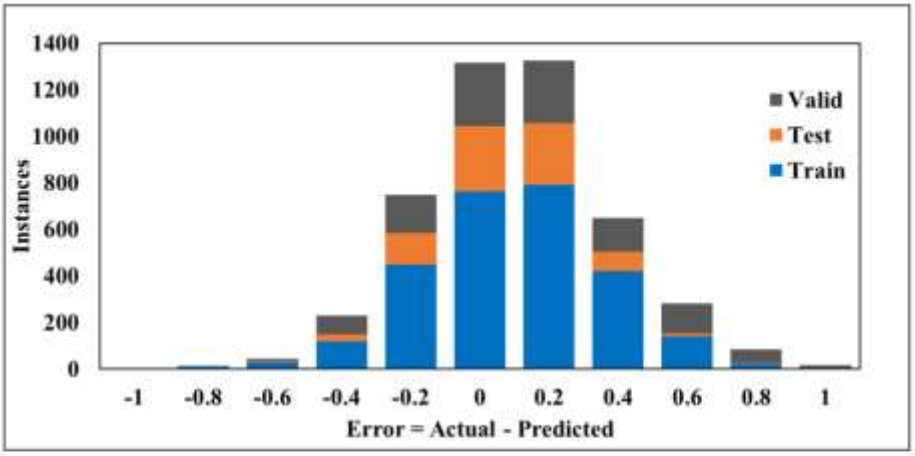

(a)

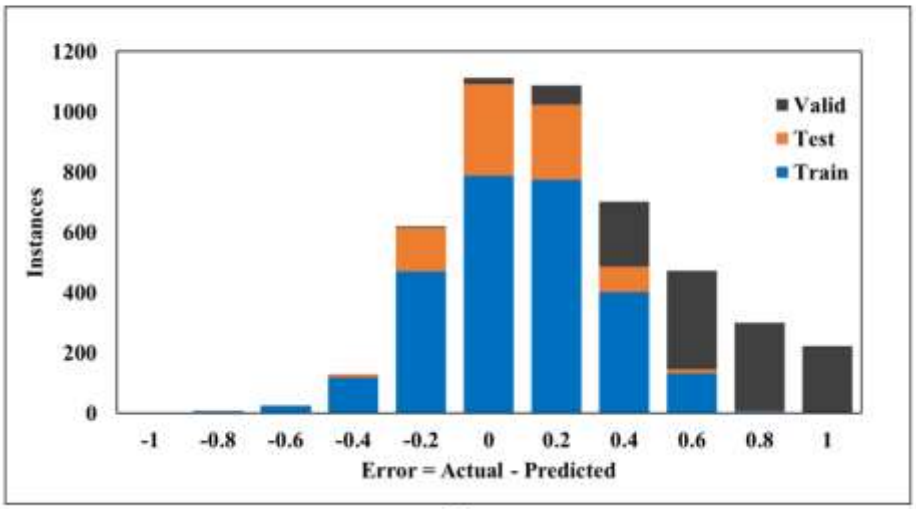

(b)

Figure 6. Error Histogram. (a) ANN model, and (b) ANFIS model.

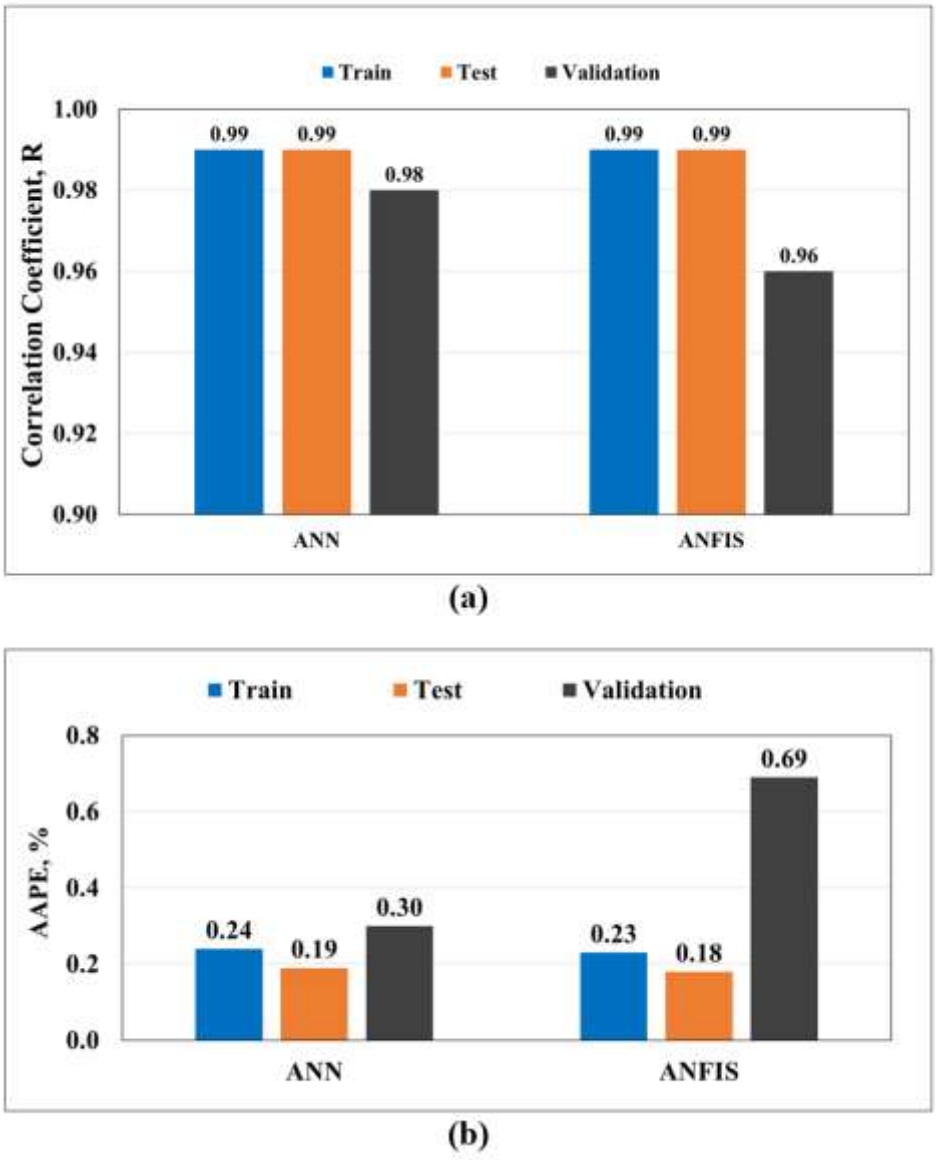

Figure 7. Models comparison. (a) Correlation coefficient (R), and (b) Average absolute percentage error (AAPE).

4. Conclusions

The equivalent circulating density (ECD) was predicted from the real-time recordings of the surface drilling sensors by employing two different machine learning techniques (ANN and ANFIS). The input drilling data are GPM, ROP, RPM, SPP, WOB, and T. The data (3570 points) was split to build the model with a 77: 23 training to testing ratio (2,743 data points for training and 827 points for testing). Another data set (1,150 points) from the same field was used for the validation process of models. Many sensitivity analyses were performed to optimize the ANN and ANFIS model parameters. The following conclusions represent the outputs from the work:

- The statistical analysis data showed a wide range for all parameters that showed the solid data-base for the two AI models.
- ANN model was optimized by one hidden layer, 15 neurons for the hidden layer, fitting network (newfit) network function, Levenberg-Marquardt backpropagation (trainlm) as a training function, and softmax as a transfer function for the model architecture.

- ANN results showed a high R of 0.99 for the training and testing, and a low AAPE of 0.24% for training and 0.19% for testing.

- ANFIS model has the optimum parameters of 0.8 for the cluster radius and 300 for the iterations number and results showed that R was 0.99 for the training and testing, and AAPE of 0.23% for training and 0.18% for testing.

- The models' validation showed a strong prediction performance for ANN and ANFIS as R was 0.98 and 0.96, and AAPE was 0.30% and 0.69% for ANN and ANFIS respectively.

- The developed empirical correlation for ECD based on the optimized ANN model showed high accuracy for predicting the ECD in real-time without the need for the ANN code.

The new contributions from this study will save time and cost for estimating ECD in the real drilling operations as the machine learning models were built based on the drilling data collected by the drilling sensors.

Author Contributions: Conceptualization, S.E.; methodology, A.AB.; software, A.AB. and H.G.; formal analysis, A.AB. and H.G.; investigation, A.AB. and H.G.; data curation, S.E.; writing—original draft preparation, A.AB. and H.G.; writing—review and editing, S.E.; supervision, S.E. All authors have read and agreed to the published version of the manuscript.

Funding: This research received no external funding.

Acknowledgments: The authors would like to thank King Fahd University of Petroleum & Minerals (KFUPM) for employing its resources in conducting this work.

Conflicts of Interest: The authors declare no conflict of interest.

Nomenclature

ECD	Equivalent circulating density
ANN	Artificial neural network
ANFIS	Adaptive network-based fuzzy interference system
R	Correlation coefficient
AAPE	Average absolute percentage error
AI	Artificial Intelligence
SVM	Support vector machine
FN	Functional networks
LLSVM	Least square support vector machine
PSO	Particle swarm optimization
FIS	Fuzzy Inference System
GA	Genetic algorithm
R^2	Coefficient of determination
MSE	Mean squared error
WOB	Weight on bit
RPM	Rotating speed in revolutions per minute
ROP	Rate of penetration
GPM	Gallon per minute
SPP	Standpipe pressure
T	Torque
Fitnet	Function fitting neural network
newfit	Create fitting network
newcf	Create cascade-forward backpropagation network

newelm	Create Elman backpropagation network
newlrn	Layer-Recurrent Network
Newdtdnn	Create distributed time delay neural network
newff	Create feedforward backpropagation network
newpr	Create pattern recognition network
newfftd	Create feedforward input-delay backpropagation network
trainbr	Bayesian regularization
trainoss	One step secant backpropagation
trainlm	Levenberg-Marquardt backpropagation
trainbfg	BFGS quasi-Newton backpropagation
traingdx	Gradient descent with momentum and adaptive learning rule backpropagation
tansig	Hyperbolic tangent sigmoid transfer function
logsig	Log-sigmoid transfer function
hardlims	Hard-limit transfer function
purelin	Linear transfer function
softmax	Softmax transfer function
tribas	Triangular basis transfer function
satlin	Saturating linear transfer function
netinv	Inverse transfer function
radbas	Radial basis transfer function

References

1. Haciislamoglu, M. 1994. Practical Pressure Loss Predictions in Realistic Annular Geometries. Paper presented at the Annual Technical Conference and Exhibition, New Orleans, Louisiana, 25-28 September. SPE-28304-MS. https://doi.org/10.2118/28304-MS.
2. Osman, E.A. and Aggour, M.A., 2003. Determination of drilling mud density change with pressure and temperature made simple and accurate by ANN. Paper presented at the Middle East Oil Show, Bahrain, 9-12 June. SPE-81422-MS. https://doi.org/10.2118/81422-MS.
3. Hemphill, T., and Ravi, K. 2011. Improved Prediction of ECD with Drill Pipe Rotation. Paper presented at the International Petroleum Technology Conference, Bangkok, Thailand, 15-17 November. IPTC-15424-MS. https://doi.org/10.2523/IPTC-15424-MS.
4. Zhang, H., Sun, T., Gao, D. and Tang, H., 2013. A new method for calculating the equivalent circulating density of drilling fluid in deepwater drilling for oil and gas. Chemistry and technology of fuels and oils, 49(5), pp.430-438.
5. Abdelgawad, K.Z., Elzenary, M., Elkatatny, S., Mahmoud, M., Abdulraheem, A. and Patil, S., 2019. New approach to evaluate the equivalent circulating density (ECD) using artificial intelligence techniques. Journal of Petroleum Exploration and Production Technology, 9(2), pp.1569-1578. https://doi.org/10.1007/s13202-018-0572-y.
6. Ataga, E., Ogbonna, J. and Boniface, O., 2012, January. Accurate estimation of equivalent circulating density during high pressure high temperature (HPHT) drilling operations. Paper presented in Nigeria Annual International Conference and Exhibition. Nigeria Annual International Conference and Exhibition, Lagos, Nigeria, 6-8 August. SPE-162972-MS. https://doi.org/10.2118/162972-MS.
7. Rommetveit, R., Odegard, S.I., Nordstrand, C., Bjorkevoll, K.S., Cerasi, P.R., Helset, H.M., Fjeldheim, M. and Havardstein, S.T., 2010, January. Drilling a challenging HP/HT well utilizing an advanced ECD management system with decision support and real-time simulations. Paper presented at the IADC/SPE Drilling Conference and Exhibition, New Orleans, Louisiana, USA, 2-4 February. SPE-128648-MS. https://doi.org/10.2118/128648-MS.
8. Erge, O., Vajargah, A. K., Ozbayoglu, M. E., & van Oort, E. 2016. Improved ECD Prediction and Management in Horizontal and Extended Reach Wells with Eccentric Drillstrings. Paper presented at the IADC/SPE Drilling

Conference and Exhibition, Fort Worth, Texas, USA, 1-3 March. SPE-178785-MS. https://doi.org/10.2118/178785-MS.

9. Hoberock, L.L., Thomas, D.C. and Nickens, H.V., 1982. Here's how compressibility and temperature affect bottom-hole mud pressure. Oil Gas J.;(United States), 80(12) 159-164.
10. Peters, E.J., Chenevert, M.E. and Zhang, C., 1990. A model for predicting the density of oil-base muds at high pressures and temperatures. SPE drilling engineering, 5(02), pp.141-148.
11. Bybee, K., 2009. Equivalent-circulating-density fluctuation in extended-reach drilling. J Petrol Technol 61:64–67. https://doi.org/10.2118/0209-0064-JPT.
12. Hemphill, T., Ravi, K., Bern, P.A. and Rojas, J., 2008. A simplified method for prediction of ECD increase with drillpipe rotation. Paper presented at the Annual Technical Conference and Exhibition, Denver, Colorado, USA, 21-24 September. SPE-115378-MS. https://doi.org/10.2118/115378-MS.
13. Ahmed, R.M., Enfis, M.S., El Kheir, H.M., Laget, M. and Saasen, A., 2010. The effect of drillstring rotation on equivalent circulation density: modeling and analysis of field measurements. Paper presented at the Annual Technical Conference and Exhibition, Florence, Italy, 19-22 September. SPE-135587-MS. https://doi.org/10.2118/135587-MS.
14. Costa, S.S., Stuckenbruck, S., Fontoura, S.A. and Martins, A.L., 2008, January. Simulation of transient cuttings transportation and ECD in wellbore drilling. Paper presented at Europec/EAGE Conference and Exhibition, Rome, Italy, 9-12 June 2008. SPE-113893-MS. https://doi.org/10.2118/113893-MS.
15. Caicedo, H. U., Pribadi, M. A., Bahuguna, S., Wijnands, F. M., & Setiawan, N. B. 2010. Geomechanics, ECD Management, and RSS to Manage Drilling Challenges in a Mature Field. Paper presented at SPE Oil and Gas India Conference and Exhibition, Mumbai, India, 20-22 January. SPE-129158-MS. https://doi.org/10.2118/129158-MS.
16. Kalogirou, S. 2003. Artificial intelligence for the modeling and control of combustion processes: a review. Progress in Energy and Combustion Science, 29(6), pp.515-566. https://doi.org/10.1016/S0360-1285(03)00058-3.
17. Shahab, M. 2000. Virtual-Intelligence Applications in Petroleum Engineering: Part 1—Artificial Neural Networks. Journal of Petroleum Technology, 52(9). https://doi.org/10.2118/58046-JPT.
18. Hag Elsafi, S., 2014. Artificial Neural Networks (ANNs) for flood forecasting at Dongola Station in the River Nile, Sudan. Alexandria Engineering Journal 53, 655–662. https://doi.org/10.1016/j.aej.2014.06.010.
19. Babikir, H.A., Abd Elaziz, M., Elsheikh, A.H., Showaib, E.A., Elhadary, M., Wu, D., and Liu, Y., 2019. Noise prediction of axial piston pump based on different valve materials using a modified artificial neural network model. Alexandria Engineering Journal 58, 1077–1087, https://doi.org/10.1016/j.aej.2019.09.010.
20. Rolon, L., Mohaghegh, S.D., Ameri, S., Gaskari, R. and McDaniel, B., 2009. Using artificial neural networks to generate synthetic well logs. Journal of Natural Gas Science and Engineering, 1(4-5), pp.118-133. https://doi.org/10.1016/j.jngse.2009.08.003.
21. Tariq, Z., Elkatatny, S., Mahmoud, M., Ali, A.Z. and Abdulraheem, A., 2017, May. A new technique to develop rock strength correlation using artificial intelligence tools. This paper was presented at the SPE Reservoir Characterisation and Simulation Conference and Exhibition. SPE-186062-MS. https://doi.org.extoljp.kfupm.edu.sa/10.2118/186062-MS.
22. Elkatatny, S., Mahmoud, M., Tariq, Z. and Abdulraheem, A., 2017. New insights into the prediction of heterogeneous carbonate reservoir permeability from well logs using artificial intelligence network. Neural Computing and Applications, 30(9), pp.2673-2683. https://doi.org/10.1007/s00521-017-2850-x.
23. Mousa, T., Elkatatny, S.M., Mahmoud, M.A. and Abdulraheem, A., 2018. Development of new permeability formulation from well log data using artificial intelligence approaches. Journal of Energy Resources Technology. https://doi.org/10.1115/1.4039270.
24. Ren, X., Hou, J., Song, S., Liu, Y., Chen, D., Wang, X., and Dou, L., 2019. Lithology identification using well logs: A method by integrating artificial neural networks and sedimentary patterns. Journal of Petroleum Science and Engineering 182, 106336. https://doi.org/10.1016/j.petrol.2019.106336.
25. Ahmed, A.S., Mahmoud, A.A., and Elkatatny, S., 2019. Fracture Pressure Prediction Using Radial Basis Function. In Proceedings of the AADE National Technical Conference and Exhibition, Denver, CO, USA, 9–10 April. AADE-19-NTCE-061.
26. Ahmed, A.S., Mahmoud, A.A., Elkatatny, S., Mahmoud, M., and Abdulraheem, A., 2019. Prediction of Pore and Fracture Pressures Using Support Vector Machine. In Proceedings of the 2019 International Petroleum

Technology Conference, Beijing, China, 26–28 March. IPTC-19523-MS. https://doi.org/10.2523/IPTC-19523-MS.

27. Elkatatny, S. and Mahmoud, M., 2018. Development of new correlations for the oil formation volume factor in oil reservoirs using artificial intelligent white box technique. Petroleum, 4(2), pp.178-186. https://doi.org/10.1016/j.petlm.2017.09.009.
28. Mahmoud, A.A., Elkatatny, S., Abdulraheem, A., and Mahmoud, M., 2017. Application of Artificial Intelligence Techniques in Estimating Oil Recovery Factor for Water Drive Sandy Reservoirs. This paper was presented at the 2017 SPE Kuwait Oil & Gas Show and Conference, Kuwait City, Kuwait, 15–18 October, SPE-187621-MS. https://doi.org/10.2118/187621-MS.
29. Mahmoud, A.A., Elkatatny, S., Chen, W., and Abdulraheem, A., 2019. Estimation of Oil Recovery Factor for Water Drive Sandy Reservoirs through Applications of Artificial Intelligence. Energies 12, 3671. https://doi.org/10.3390/en12193671.
30. Elkatatny, S., Al-AbdulJabbar, A., and Mahmoud, A.A., 2019. New Robust Model to Estimate the Formation Tops in Real-Time Using Artificial Neural Networks (ANN). Petrophysics 60, 825–837. https://doi.org/10.30632/PJV60N6-2019a7.
31. Al-Abduljabbar, A., Gamal, H. and Elkatatny, S. 2020. Application of artificial neural network to predict the rate of penetration for S-shape well profile. Arab J Geosci 13, 784. https://doi.org/10.1007/s12517-020-05821-w.
32. Gamal, H., Elkatatny, S. and Abdulraheem, A., 2020, November. Rock Drillability Intelligent Prediction for a Complex Lithology Using Artificial Neural Network. Paper presented in Abu Dhabi International Petroleum Exhibition & Conference, Abu Dhabi, UAE, 9-12 November. SPE-202767-MS. https://doi.org/10.2118/202767-MS.
33. Mahmoud, A.A., Elkatatny, S., Al-AbdulJabbar, A., Moussa, T., Gamal, H. and Shehri, D.A., 2020, September. Artificial Neural Networks Model for Prediction of the Rate of Penetration While Horizontally Drilling Carbonate Formations. In 54th US Rock Mechanics/Geomechanics Symposium. American Rock Mechanics Association. ARMA-2020-1694.
34. Mahmoud, A.A., Elkatatny, S., Abdulraheem, A., Mahmoud, M., Ibrahim, O., and Ali, A., 2017. New Technique to Determine the Total Organic Carbon Based on Well Logs Using Artificial Neural Network (White Box). This paper was presented at the SPE Kingdom of Saudi Arabia Annual Technical Symposium and Exhibition, Dammam, Saudi Arabia, 24–27 April. SPE-188016-MS. https://doi.org/10.2118/188016-MS.
35. Mahmoud, A.A., Elkatatny, S., Ali, A., Abouelresh, M., and Abdulraheem, A., 2019. New Robust Model to Evaluate the Total Organic Carbon Using Fuzzy Logic. This paper was presented at the SPE Kuwait Oil & Gas Show and Conference, Mishref, Kuwait, 13–16 October. SPE-198130-MS. https://doi.org/10.2118/198130-MS.
36. Mahmoud, A.A., Elkatatny, S., Mahmoud, M., Abouelresh, M., Abdulraheem, A., and Ali, A., 2017. Determination of the total organic carbon (TOC) based on conventional well logs using artificial neural network. International Journal of Coal Geology 179, 72–80. https://doi.org/10.1016/j.coal.2017.05.012.
37. Mahmoud, A.A., Elkatatny, S., and Al-Shehri, D., 2020. Application of Machine Learning in Evaluation of the Static Young's Modulus for Sandstone Formations. Sustainability 12(5). https://doi.org/10.3390/su12051880.
38. Mahmoud, A.A., Elkatatny, S., Ali, A., and Moussa, T., 2019. Estimation of Static Young's Modulus for Sandstone Formation Using Artificial Neural Networks. Energies 12, 2125, https://doi.org/10.3390/en12112125.
39. Tariq, Z., Elkatatny, S., Mahmoud, M. and Abdulraheem, A., 2016, November. A holistic approach to develop new rigorous empirical correlation for static Young's modulus. This paper was presented at Abu Dhabi International Petroleum Exhibition & Conference. Abu Dhabi, UAE, 7-10 November. SPE-183545-MS. https://doi.org/10.2118/183545-MS.
40. Elkatatny, S., Mahmoud, M., Mohamed, I. and Abdulraheem, A., 2018. Development of a new correlation to determine the static Young's modulus. Journal of Petroleum Exploration and Production Technology, 8(1), pp.17-30. https://doi:10.1007/s13202-017-0316-4.
41. Elkatatny, S., Tariq, Z., Mahmoud, M., Mohamed, I. and Abdulraheem, A., 2018. Development of new mathematical model for compressional and shear sonic times from wireline log data using artificial intelligence neural networks (white box). Arabian Journal for Science and Engineering, 43(11), pp.6375-6389. https://doi.org/10.1007/s13369-018-3094-5.
42. Tariq, Z., Elkatatny, S., Mahmoud, M., Ali, A.Z. and Abdulraheem, A., 2017, June. A new approach to predict failure parameters of carbonate rocks using artificial intelligence tools. This paper was presented at SPE Kingdom of Saudi Arabia Annual Technical Symposium and Exhibition. Dammam, Saudi Arabia, 24-27 April. SPE-187974-MS. https://doi.org/10.2118/187974-MS.

43. Alsaihati, A., Elkatatny, S., Mahmoud, A.A. and Abdulraheem, A., 2020. Use of Machine Learning and Data Analytics to Detect Downhole Abnormalities While Drilling Horizontal Wells, With Real Case Study. Journal of Energy Resources Technology, 143(4). https://doi.org/10.1115/1.4048070.
44. Arehart, R.A., 1990. Drill-bit diagnosis with neural networks. SPE Computer Applications 2, 24–28. https://doi.org/10.2118/19558-PA.
45. Abdelgawad, K., Elkatatny, S., Moussa, T., Mahmoud, M., and Patil, S., 2018. Real Time Determination of Rheological Properties of Spud Drilling Fluids Using a Hybrid Artificial Intelligence Technique. Journal of Energy Resources Technology. https://doi.org/10.1115/1.4042233.
46. Elkatatny, S.M., 2017. Real Time Prediction of Rheological Parameters of KCl Water-Based Drilling Fluid Using Artificial Neural Networks. Arabian Journal of Science and Engineering 42, 1655–1665. https://doi.org/10.1007/s13369-016-2409-7.
47. Alsabaa, A., Gamal, H., Elkatatny, S. and Abdulraheem, A., 2020. Real-Time Prediction of Rheological Properties of Invert Emulsion Mud Using Adaptive Neuro-Fuzzy Inference System. Sensors, 20(6), p.1669. https://doi.org/10.3390/s20061669.
48. Alsabaa A, Gamal H, Elkatatny SM, Abdulraheem A. Real-Time Prediction of Rheological Properties of All-Oil Mud Using Artificial Intelligence. This paper was presented at the 54th US Rock Mechanics/Geomechanics Symposium 2020 Sep 18. American Rock Mechanics Association. ARMA-2020-1645.
49. Elkatatny, S., Tariq, Z. and Mahmoud, M., 2016. Real time prediction of drilling fluid rheological properties using Artificial Neural Networks visible mathematical model (white box). Journal of Petroleum Science and Engineering, 146, pp.1202-1210. https://doi.org/10.1016/j.petrol.2016.08.021.
50. Ahmadi, M.A., 2016. Toward reliable model for prediction Drilling Fluid Density at wellbore conditions: A LSSVM model. Neurocomputing, 211, pp.143-149. https://doi.org/10.1016/j.neucom.2016.01.106.
51. Ahmadi, M.A., Shadizadeh, S.R., Shah, K. and Bahadori, A., 2018. An accurate model to predict drilling fluid density at wellbore conditions. Egyptian Journal of Petroleum, 27(1), pp.1-10. http://dx.doi.org/10.1016/j.ejpe.2016.12.002.
52. Alkinani, H.H., Al-Hameedi, A.T.T., Dunn-Norman, S., Al-Alwani, M.A., Mutar, R.A. and Al-Bazzaz, W.H., 2019, October. Data-Driven Neural Network Model to Predict Equivalent Circulation Density ECD. Paper presented at the Gas & Oil Technology Showcase and Conference, Dubai, UAE, 21-23 October. SPE-198612-MS. https://doi.org/10.2118/198612-MS.
53. Rahmati, A.S. and Tatar, A., 2019. Application of Radial Basis Function (RBF) neural networks to estimate oil field drilling fluid density at elevated pressures and temperatures. Oil & Gas Science and Technology–Revue d'IFP Energies nouvelles, 74, p.50.
54. Bello, O., Holzmann, J., Yaqoob, T. and Teodoriu, C. 2015. Application of Artificial Intelligence Methods in Drilling System Design and Operations: A Review of the State of The Art". Journal of Artificial Intelligence and Soft Computing Research, 5(2), pp.121-139. https://Doi.org/10.1515/jaiscr-2015-0024.
55. Abbas, A., Rushdi, S., Alsaba, M. and Al Dushaishi, M. 2019. Drilling Rate of Penetration Prediction of High-Angled Wells Using Artificial Neural Networks. Journal of Energy Resources Technology, 141(11). https://doi.org/10.1115/1.4043699.
56. Cevik, A., Sezer, E.A., Cabalar, A.F. & Gokceoglu, C. 2011. Modeling of the uniaxial compressive strength of some clay-bearing rocks using neural network. Applied Soft Computing, 11, 2587–2594, https://doi.org/10.1016/j.asoc.2010.10.008.
57. Lippman, R.P. & Lippman, R.P. 1987. An Intrduction to Computing with Neural Nets. In: Mag, A. (ed.) IEEE ASSP Magazine. IEEE, 4–22., https://doi.org/10.1109/MASSP.1987.1165576.
58. Graves, A., Liwicki, M., Fernandez, S., Bertolami, R., Bunke, H. & Schmidhuber, J. 2009. A Novel Connectionist System for Unconstrained Handwriting Recognition. IEEE Transactions on Pattern Analysis and Machine Intelligence, 31, 855–868, https://doi.org/10.1109/TPAMI.2008.137.
59. Nakamoto, P. Neural Networks and Deep Learning: Deep Learning Explained to Your Granny a Visual Introduction for Beginners Who Want to Make Their Own Deep Learning Neural Network (Machine Learning); CreateSpace Independent Publishing Platform: Scotts Valley, CA, USA, 2017.
60. Jang, J.-S.R. (1993). "ANFIS: adaptive-network-based fuzzy inference system". IEEE Transactions on Systems, Man and Cybernetics. 23 (3): 665–685. https://psycnet.apa.org/doi/10.1109/21.256541.
61. Abraham A. 2005. Adaptation of Fuzzy Inference System Using Neural Learning. In: Nedjah N., Macedo Mourelle L. (eds) Fuzzy Systems Engineering. Studies in Fuzziness and Soft Computing, vol 181. Springer, Berlin, Heidelberg. https://doi.org/10.1007/11339366_3.

Figures

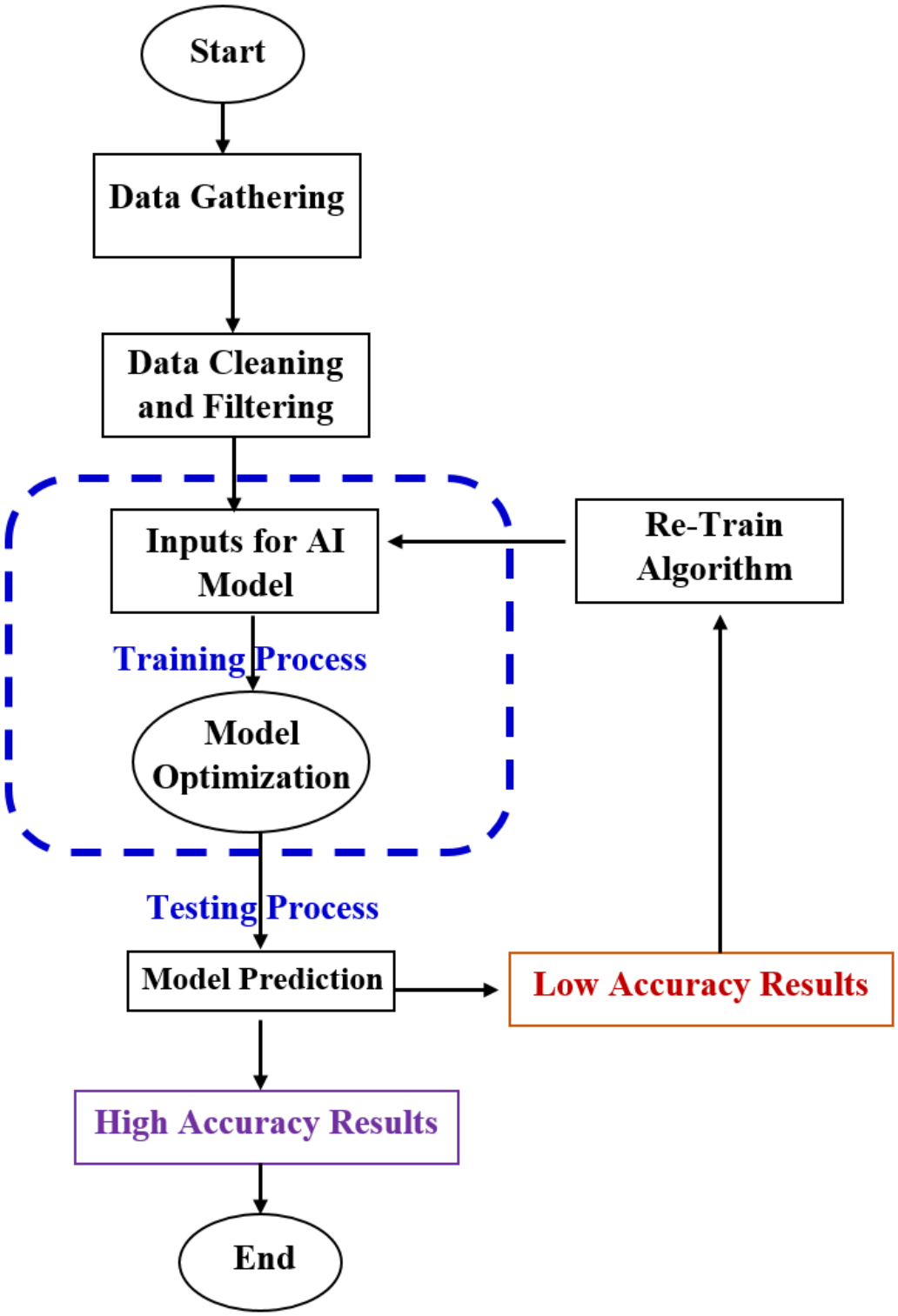

Figure 1

Processing flow chart for ECD AI models.

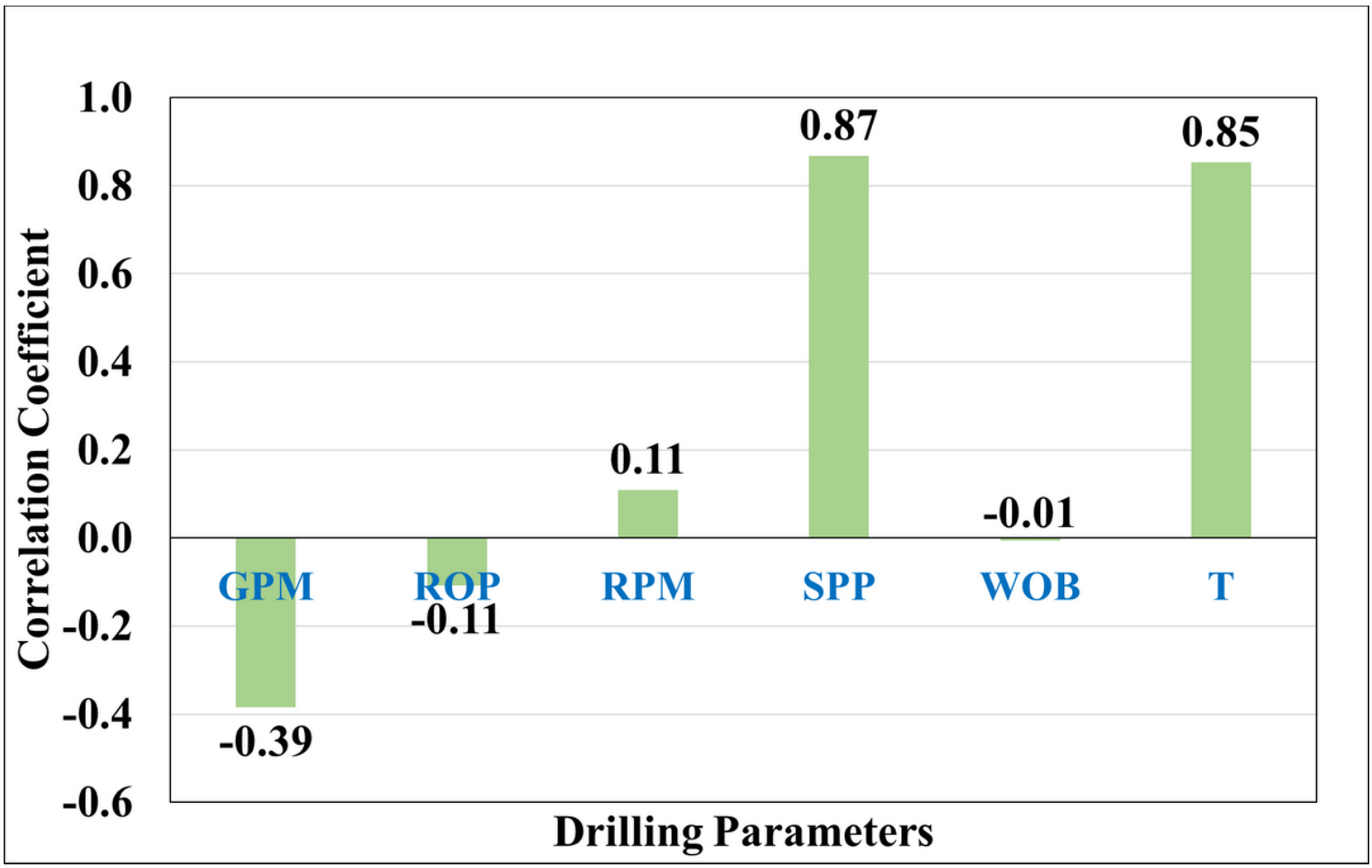

Figure 2

The correlation coefficients between the inputs and ECD after data preprocessing

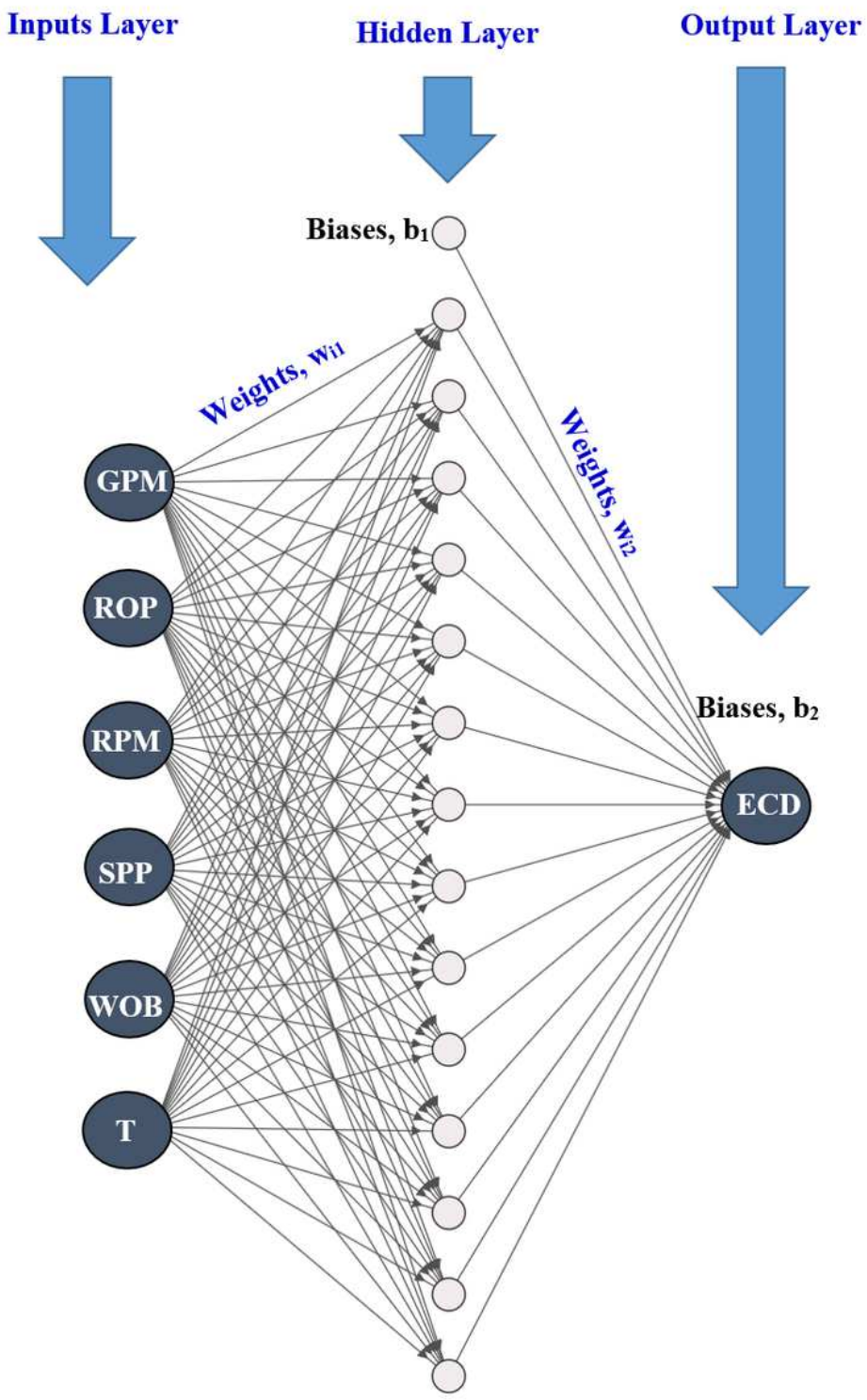

Figure 3

The architecture of the developed ANN model.

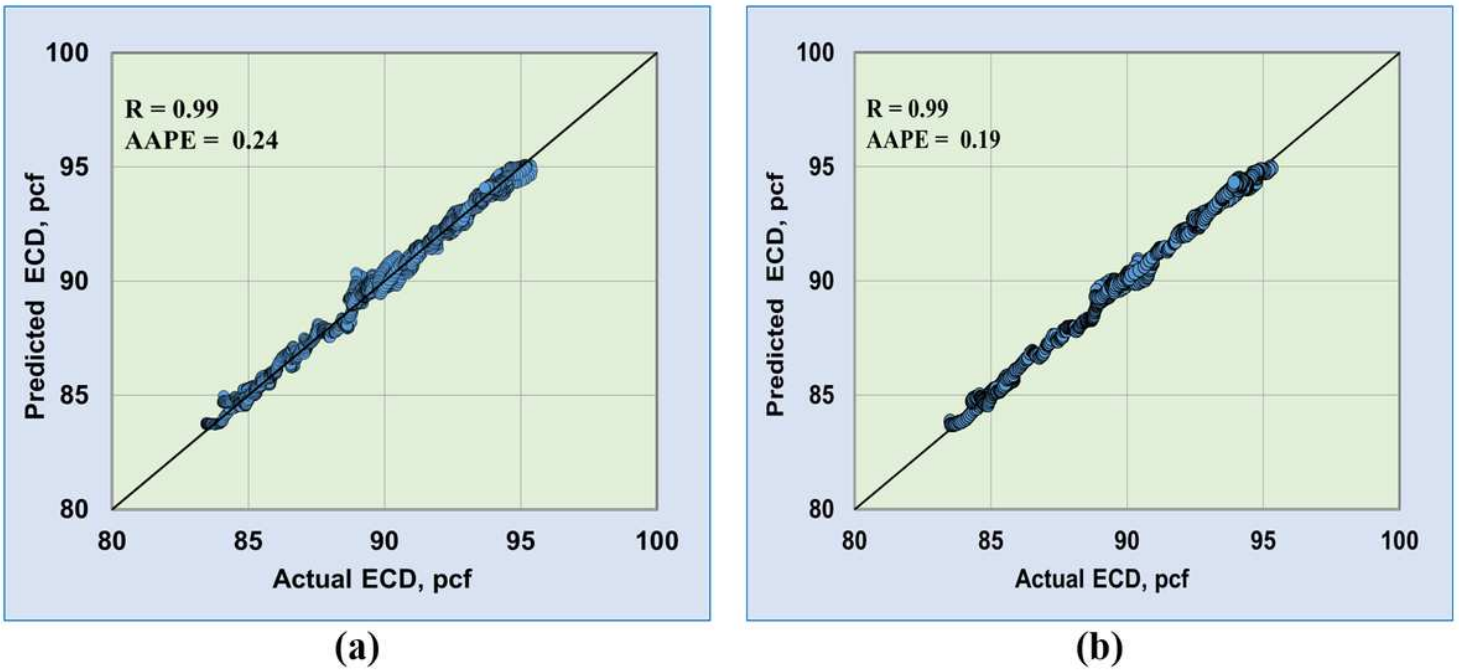

Figure 4

Cross-plots between the predicted and actual ECD results from the developed ANN model. (a) training process, and (b) testing process.

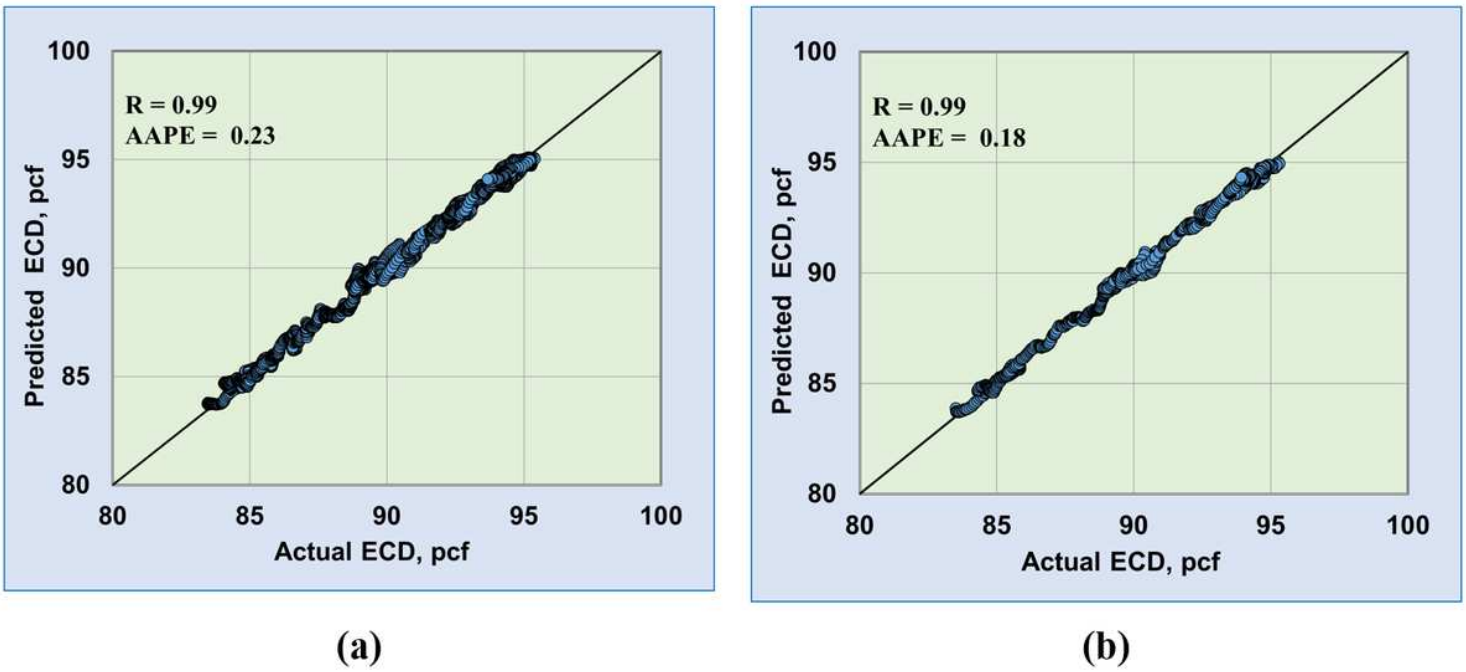

Figure 5

Cross-plots between the predicted and actual ECD results from the developed ANFIS model. (a) training process, and (b) testing process.

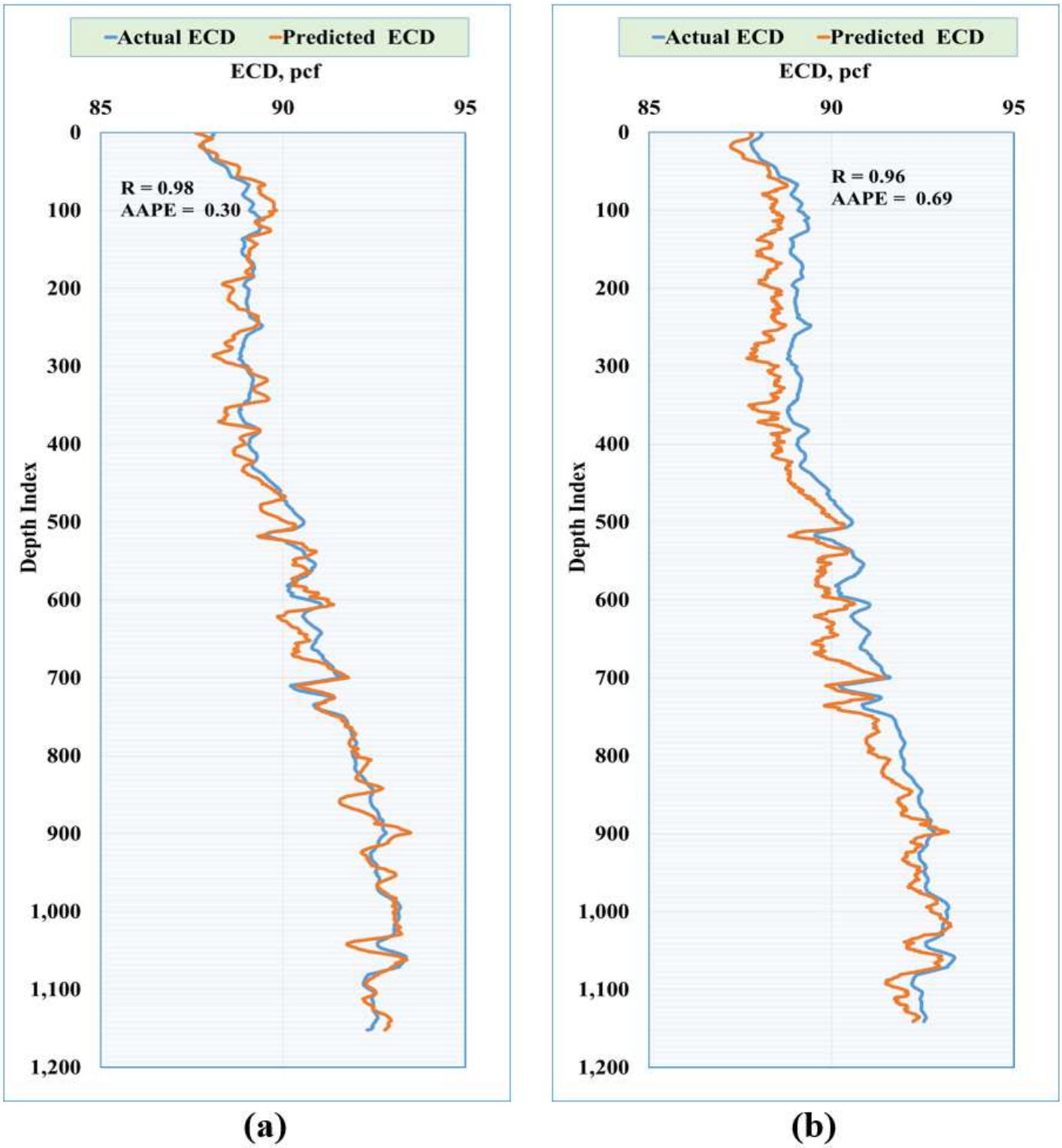

Figure 6

ECD Profile for the validation data set. (a) ANN model, and (b) ANFIS model.

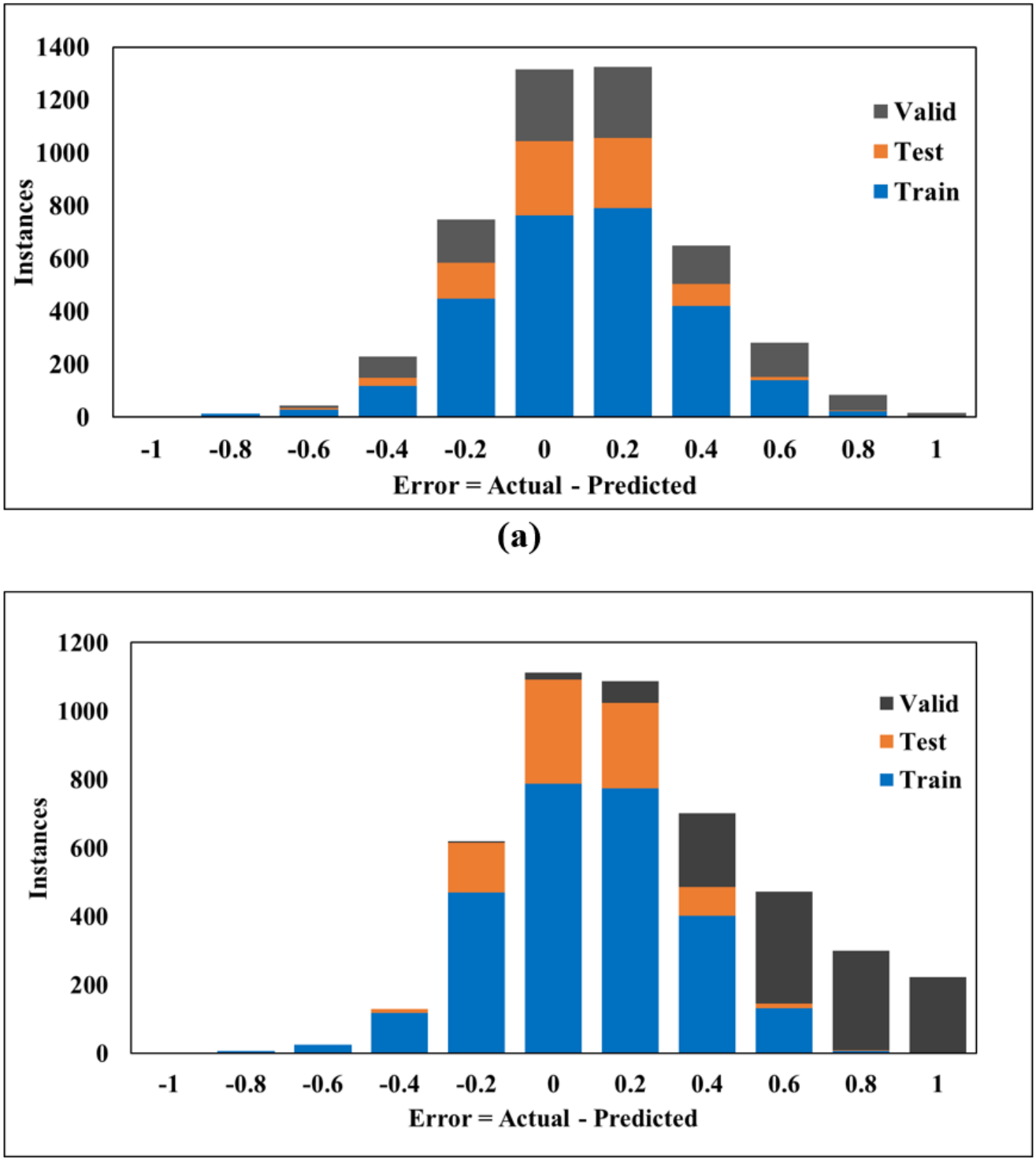

Figure 7

Error Histogram. (a) ANN model, and (b) ANFIS model.

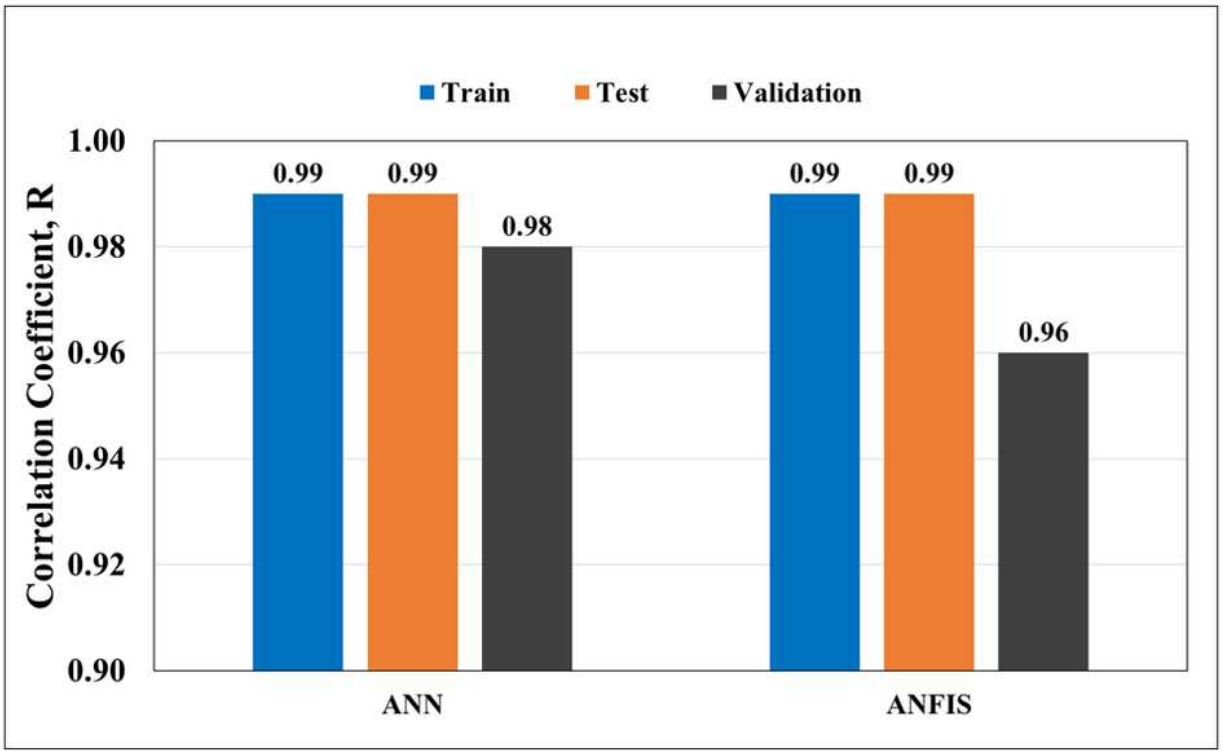

(a)

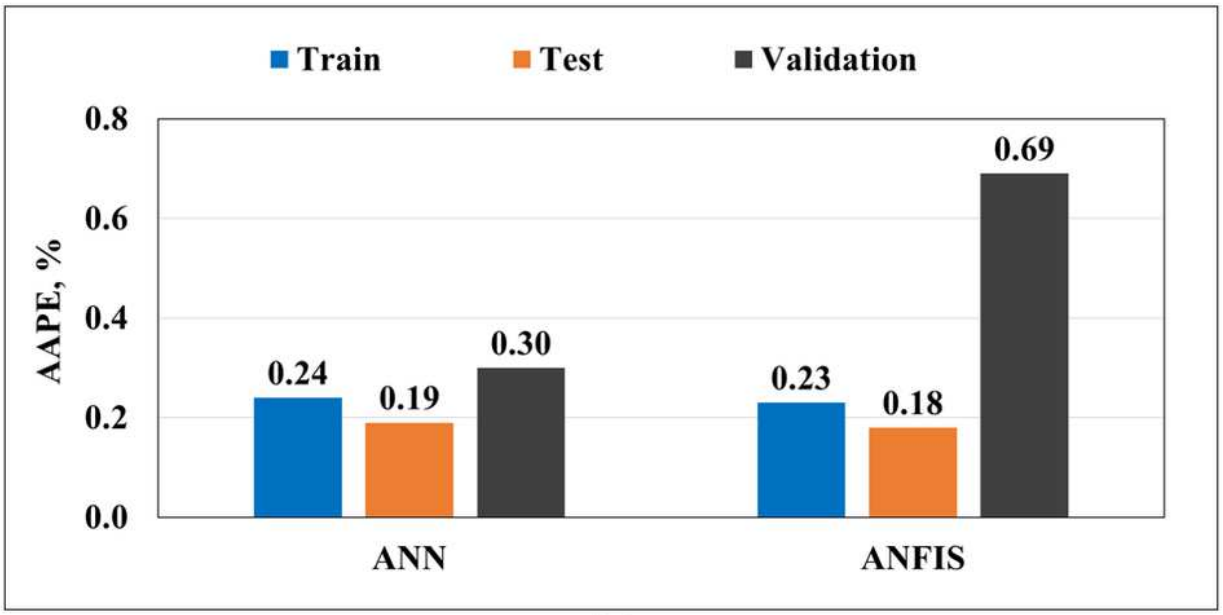

(b)

Figure 8

Models comparison. (a) Correlation coefficient (R), and (b) Average absolute percentage error (AAPE).